วิศวกรรมสาร มข. ปีที่ 37 ฉบับที่ 1 (65 - 70) มกราคม - มีนาคม 2553 บทความวิจัย
KKU Engineering Journal Vol.37 No.1 (65 - 70) January - February 2010

Effect of bearing sleeve lead-in chamfer, and parallelism on tolerance ring installation

Piriyakorn Jirawattanakasem [1] and Sujin Bureerat [*2]

Abstract

Tolerance-ring (T-ring) installation is one of the assembly processes used to assemble a bearing cartridge that consists of one or two miniature ball bearings, a center shaft and a bearing sleeve to the bore of a hard disk drive (HDD) actuator arm. This process is widely used due to its cost effectiveness, repeatability of assembly, ease of rework, short cycle time and fulfillment of a resonance performance design requirement. In this paper, the finite element (FE) model of a T-ring installation process is proposed. The FE computational result of push-in force is compared to that from experiment, and it is found to be acceptable. It is also found that the solid elements provide better computational results than the shells. Then this model is further used to determine the main contributor to push-in force. It is found that the bearing sleeve parallelism has significant impact on the process but it is somewhat unaffected by the change in the lead-in chamfer.

Keywords: Finite element analysis, Tolerance-ring installation, Hard disk drive, Contact analysis.

[1] Post graduated Students, Department of Mechanical Engineering, Khon Kaen University, Khon Kaen, 40002, E-mail: piriyakornj@hotmail.com

[*2] Associate Professor, Department of Chemical Engineering, Khon Kaen University, Khon Kaen, 40002, E-mail: sujbur@kku.ac.th

1. Introduction

Tolerance rings are used in hard disk drive (HDD) manufacturing due to their low cost, ease to rework, repeatability of assembly, high cycle time and fulfillment of a resonance constraint.

This application is to mount a bearing cartridge, which consists of one or two miniature ball bearings, and a center shaft with or without a cartridge sleeve. A view of the assembly is shown in Fig. 1.

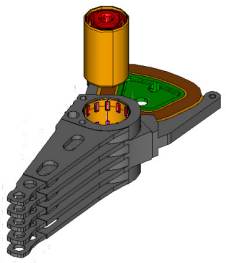

Fig. 1 *Picture of tolerance ring assembly*

A tolerance ring installation process starts by firstly placing an E-block on the fixture of a T-ring machine then putting a tolerance ring in the E-block. The next step is to place a bearing cartridge on the movable datum and seat on the outer sleeve. The top clamp of the T-ring machine presses on this outer sleeve until it reaches the hard stop datum at the bottom. Once the bearing cartridge has passed through the tolerance ring's bumps, plastic deformation, which occurred during the process, remains while some of the elastic deformations recover such that the contacting surfaces between the parts conform to each other.

The aim of this work is to initiate a model to predict the contact force during installation and to determine the major contributor of this contact force. In the present work, the tolerance ring installation process is studied by performing a large-deformation, explicit dynamic finite element analysis (FEA) using a commercial program. The E-block, tolerance ring and outer sleeve are opted as the model to be studied. The top clamp of the Tolerance ring machine is moving with a constant velocity of 18 mm/s from top to bottom.

2. Finite Element Analysis

The use of finite element analysis for material processing techniques, particularly for those involving contact mechanics, has been studied for many years (Zhi-Hua Zhong, 1993; Wriggers P, 2006; Jaroslav Mackerle, 1998; Piela A. and Grosman F., 1996; F. H. Lin and A. A. Tseng, 1998; Nagi Elabbasi, Jung-Wuk Hong and Klaus-Jürgen Bathe, 2004; Wang Xucheng, Chang Liangming and Cen Zhangzhi, 1990). Much research work towards the finite element procedures for contact-impact mechanics has been investigated (Zhi-Hua Zhong, 1993; Wriggers P, 2006; F. H. Lin and A. A. Tseng, 1998; Nagi Elabbasi, Jung-Wuk Hong and Klaus-Jürgen Bathe, 2004). A contact system of multiple deformable bodies can be thought of as a system having a static or dynamic equilibrium state such that contact constraints are imposed on the surfaces of the bodies contacting each other. The equation of motion of a body occupying a space domain Ω can be written as (Zhi-Hua Zhong, 1993)

$$\frac{\partial \sigma_{ji}(\mathbf{x},t)}{\partial x_j} + b_i(\mathbf{x},t) = \rho a_i(\mathbf{x},t)$$

for i = 1, …, 3 and j = 1, …, 3 (1)

where **x** is a point on Ω, σ_{ji} is a Cauchy stress component, **b** is a body force vector, ρ is material

density, and **a** is an acceleration vector. The boundary of the body Ω can be defined as Γ, and it is divided into three distinct parts as

$$\Gamma = \Gamma_d \cup \Gamma_f \cup \Gamma_c \tag{2}$$

where Γ_d is the boundary part having prescribed displacements, Γ_f is the boundary part that has prescribed forces, and Γ_c the boundary part contacting to other bodies. The prescribed boundary conditions can be written as

$$\begin{aligned} u_i(\mathbf{x},t) &= \overline{u}_i(\mathbf{x},t); \mathbf{x} \in \Gamma_d \\ \sigma_{ij}(\mathbf{x},t)N_j &= \overline{q}_i(\mathbf{x},t); \mathbf{x} \in \Gamma_f \end{aligned} \tag{3}$$

where $\overline{u}_i$ and $\overline{q}_i$ are prescribed displacement and boundary traction components respectively. N_j is the component of an outward normal vector at **x** on Γ_f. The initial conditions for displacement (**u**) and velocity (**v**) are also needed as:

$$\begin{aligned} \mathbf{u}(\mathbf{x},0) &= \overline{\mathbf{u}}(\mathbf{x}); \mathbf{x} \in \Omega \\ \mathbf{v}(\mathbf{x},0) &= \overline{\mathbf{v}}(\mathbf{x}); \mathbf{x} \in \Omega \end{aligned} \tag{4}$$

where $\overline{\mathbf{u}}$ and $\overline{\mathbf{v}}$ are prescribed displacement and velocity respectively. The contact constraints are assigned in such a way that the contact stress should be negative (or compressive) whereas there is no penetration between bodies. The contact constraints on Γ_f can be expressed as:

$$\begin{aligned} g(\mathbf{x},t) &= g(\mathbf{x},0) - \mathbf{u}(\mathbf{x},t)\cdot\mathbf{N} \geq 0; \mathbf{x} \in \Gamma_c \\ \overline{\mathbf{q}}_c(x,t)\cdot\mathbf{N} &\leq 0; \mathbf{x} \in \Gamma_c \end{aligned} \tag{5}$$

where g is the gap between contact surfaces, and $\mathbf{q}_c$ is the contact traction.

By using a finite element approach, the mathematical model (1) to (5) can be simplified to the matrix form of the system of second order differential equations. Using implicit and explicit time integration techniques, the system of differential equations can then be solved. Several numerical schemes dealing with contact mechanic finite element analysis have been proposed such as the Lagrange multiplier method, the augment Lagrangian method, and the penalty method. These methods have been implemented on numerous real world contact problems with success.

In this study, the simulation model is solved by explicit time integration techniques and the Lagrange element method (part to part contact). The augment Lagrangian method is used to deal with contact constraints.

3. Tolerance Ring Model

The five parts involved in the tolerance ring installation process are modeled; namely, the E-block housing hole, the outer sleeve of the bearing cartridge, the tolerance ring, the top clamp and the bottom datum which supports the tolerance ring.

The E-block housing is meshed using 3-dimensional brick elements while the outer sleeve and the bottom datum are set as rigid bodies. Two types of elements, shells and solids, are used for meshing the T-ring in order to investigate the effect of using different element types.

During the tolerance ring installation, the arm is first placed on the fixture of the T-Ring machine. The ring is then put inside the arm bore while seating on the bottom datum. The bearing cartridge is placed on the movable supporting shaft and pressed by the top clamp with a constant velocity. This top clamp presses on the outer sleeve

of the bearing cartridge until it reaches the stopper at the bottom (see Fig.2).

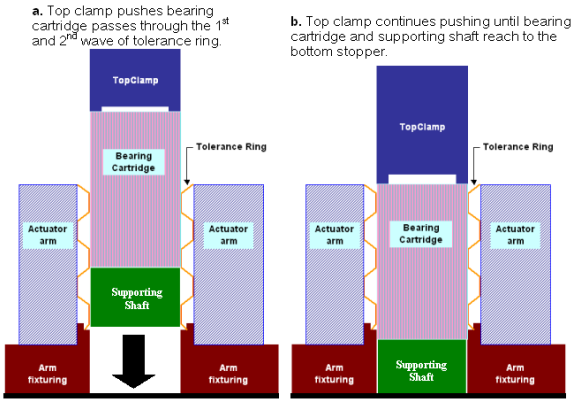

Fig. 2 *Tolerance ring installation process*

The bottom datum is made of stainless steel and is hardly deformed during the tolerance ring installation because it is used to support only the tolerance ring. Thus, it is simulated as a rigid body. The outer sleeve and tolerance ring are made of stainless steel while the arm is made of aluminum. The material models defined in the analysis are bilinear kinematics hardening. The results of the reaction force at the outer sleeve and tolerance ring are evaluated. The material properties used in the simulation are listed in Table 1.

Table 1 *Material Properties used in the Finite Element Analysis*

Material Properties	Type of Material	
	Stainless steel	*Aluminum*
Elastic modulus, E (MPa)	190,000	71,016
Yield stress, Y (MPa)	206	275
Poisson ratio	0.32	0.33
Mass density (kg/m^3)	7889	2700

All the elements used in the solid elements analysis are eight-node brick elements. To reduce the computational time, only the outer sleeve, which is one of the components of the bearing cartridge, is used in the model. As for the arm, it is focused only on the bearing bore area while the arm tip and fantail area are excluded. Meshing of the structure is illustrated in Fig. 3.

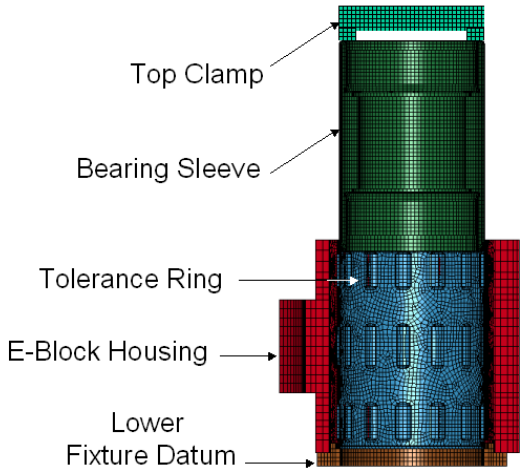

Fig. 3 *Finite element grids of a tolerance ring installation (all parts are solid elements)*

4. Simulation Results

Fig. 4 displays the value of push-in force from FEA model of a tolerance ring. The lower graph is obtained from a model using solid elements whereas the upper graph is from a model using shells.

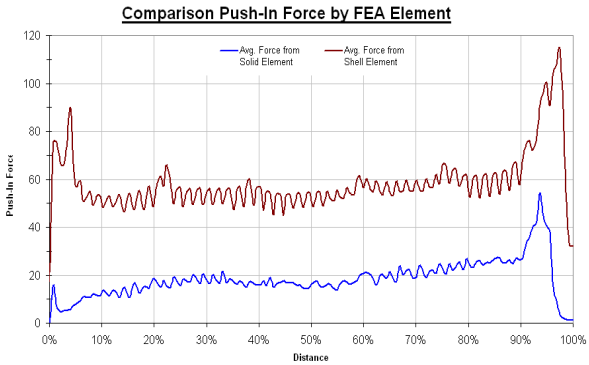

Fig. 4 *Push-in force comparison between Shell and Solid elements*

The push-in force from experimentation is shown as a black line compared to the solid elements line shown as a blue line in Fig. 5.

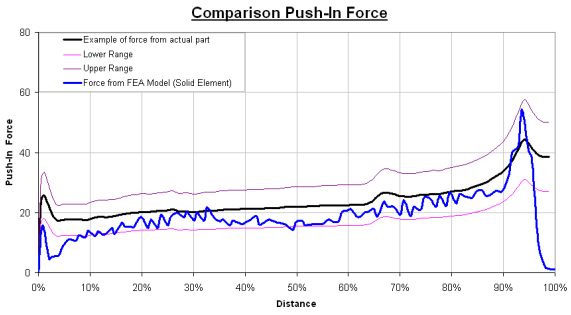

Fig. 5 *Push-in force graph of the actual part*

From the figures, it can be seen that the graph of solid elements (blue line) agrees well with that from the testing results and most of the blue line values are within +/-30% tolerance of the testing results. The push-in force curve from testing is smoother than the computational results because the data acquisition rate of the testing results is higher than what is given in simulation.

When using solid elements during the contact finite element process, the thickness of the ring is taken into consideration. Nevertheless, when using shell elements that have a higher-order polynomial function compared to solids, the ring is treated as having zero thickness although the effect of shell thickness is included in the mass and stiffness matrices. This means that the actual dimensions of parts should be taken into account when performing finite element contact analysis.

This simulation model is used to perform DoE experiments by varying bearing sleeve dimension, lead-in chamfer and parallelism. The result shows the lead-in chamfer is not the major contributor to the push-in force but the bearing sleeve parallelism is (see Figs. 6,7).

Term	Coef	SE Coef	T	P
Constant	6.5322	1.0619	6.151	0.000
Lead-In Chamfer	0.9071	0.5642	1.608	0.116
Sleeve Parallelism	11.3887	2.2283	5.111	0.000
Lead-In Chamfer*Lead-In Chamfer	0.8771	0.3016	2.908	0.006
Sleeve Parallelism*Sleeve Parallelism	-2.3060	1.0705	-2.154	0.037
Lead-In Chamfer*Sleeve Parallelism	1.3455	0.4370	3.079	0.004

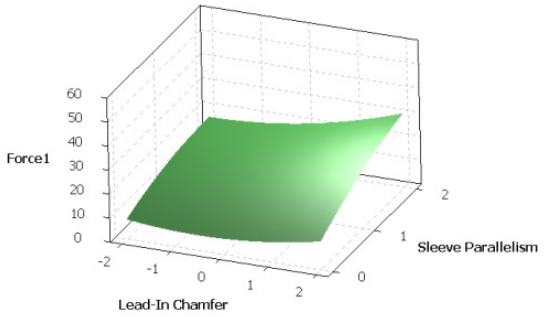

Fig. 6 *Regression & Surface Plot of Force1*

Estimated Regression Coefficients for **Force2**

Term	Coef	SE Coef	T	P
Constant	30.4573	2.3538	12.939	0.000
Lead-In Chamfer	-0.3500	1.2505	-0.280	0.781
Sleeve Parallelism	29.8938	4.9392	6.052	0.000
Lead-In Chamfer*Lead-In Chamfer	0.4387	0.6684	0.656	0.516
Sleeve Parallelism*Sleeve Parallelism	-12.2581	2.3727	-5.166	0.000
Lead-In Chamfer*Sleeve Parallelism	-0.3625	0.9687	-0.374	0.710

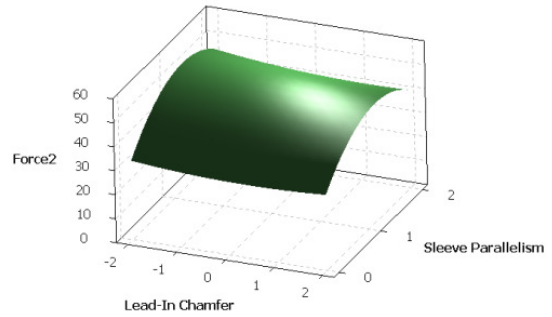

Fig. 7 *Regression & Surface Plot of Force2*

Fig. 8 displays the plastic stain profile comparison between the good bearing vs the worst bearing sleeve parallelism. It can be seen that the deformed tolerance ring bumps are observed on only one portion. This results because while the top clamp is pressing on the top of the bearing sleeve, the bearing sleeve will be tilted causing only one edge of bearing sleeve to drag along the tolerance ring. A higher push-in force occurs with this phenomenon.

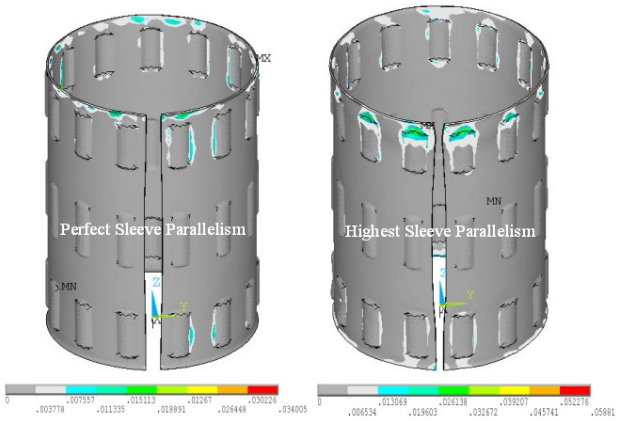

Fig. 8 *Plastic Stain Profile*

5. Conclusions and Discussion

The finite element model of a T-ring installation process is proposed. Solid and shell elements are employed to model the T-ring. The computational results obtained from both finite element formulations are compared with those from experimentation. It is found that solid elements give better and more reasonable results.

The Simulation results show that the bearing sleeve parallelism is the major contributor to an increase in the push-in force. Therefore, the bearing sleeve and top clamp parallelism dimension must be tightly controlled to ensure that the bearing sleeve is perpendicularly pushed into the tolerance ting in order to avoid a high push-in force and resultant damages to the bearing structure.

6. Acknowledgement

This study is supported by Cooperate Project between National Electronics and Computer Technology Center (NECTEC) and Seagate Technology (Thailand) via Industry/University Cooperative Research Center (I/UCRC) in HDD Component, Khon Kaen University.

7. References

F. H. Lin and A. A. Tseng, A finite element analysis of elasto-plastic contact problems in metal forming, Materials and Design, Volume 19, Issue 3, 1 June 1998, Pages 99-108

Jaroslav Mackerle, Finite element methods and material processing technology, an addendum (1994-1996), Engineering Computations, Aug 1998 Volume: 15 Issue: 5 Page: 616 – 690

Klaus-Jürgen Bathe, Finite Element Procedures, Prentice Hall, Englewood Cliffs, 1996

Nagi Elabbasi, Jung-Wuk Hong and Klaus-Jürgen Bathe, On the Reliable Solution of Contact Problems in Engineering Design, International Journal of Mechanics and Materials in Design Volume 1, Number 1 / March, 2004

Piela A.; Grosman F., Spatial modelling of swaging process using finite element method applied to axially-symmetrical problems, Journal of Materials Processing Technology, Volume 60, Number 1, 15 June 1996, pp. 517-522(6)

Wang Xucheng, Chang Liangming and Cen Zhangzhi, Effective numerical methods for elasto-plastic contact problems with friction, Acta Mechanica Sinica, Volume 6, Number 4 / November, 1990

Wriggers P, Computational contact mechanics, Springer, Berlin, 2006

Zhi-Hua Zhong, Finite element procedures for contact-impact problems, Oxford science publication, Oxford, 1993